THE UNIVERSITY OF MICHIGAN

College of Engineering

Department of Mechanical Engineering

Cavitation and Multiphase Flow Laboratory

Report No. 03371-1-T

IMPACT AND CAVITATION EROSION AND MATERIAL MECHANICAL PROPERTIES

(Submitted for Journal Publication)

by

F. G. Hammitt

Financial Support Provided by:

NSF Grant GK 13081

November 1969

ABSTRACT

The mechanisms of mechanical cavitation and liquid impingement damage are reviewed. In the light of available experimental and photographic evidence it is concluded that the predominant mechanisms in real flow situations of mechanical cavitation damage and liquid impingement damage are very probably the same, i.e. liquid jet impingement in both cases. Numerical data relating to the microjet diameter and velocity in the cavitation case is presented.

A comprehensive data set involving only metallic materials, but with tests conducted in several types of cavitation facilities as well as liquid impact facilities, is used to obtain a relatively simple best fit correlation in terms of conventional mechanical properties of materials. It is concluded that no very precise correlation of this type with general applicability even for metallic materials is possible, and that a standard error of estimate factor for a new material is of the order of 2.5.

TABLE OF CONTENTS

LIST OF FIGURES

LIST OF TABLES

IMPACT AND CAVITATION EROSION AND MATERIAL MECHANICAL PROPERTIES

I. INTRODUCTION

The detailed mechanisms whereby cavitation or liquid impingement cause damage to even the strongest of materials are undoubtedly extremely complex. In the case of either phenomenon, mechanical effects are apparently usually predominant, although in both cases corrosive effects are also more or less important. While either phenomenon as encountered in the field may often include both significant corrosive and mechanical influences, the combined phenomena in the present state of the art seems too complex for useful basic study. Hence, most laboratory investigations of cavitation or liquid impingement have been conducted with material-fluid combinations and intensities such that mechanical effects predominate. The present paper concerns only the basic mechanisms involved in mechanical attack from either cavitation or liquid impingement. In addition, the correlation of volume loss rates from cavitation or liquid impingement with material mechanical properties is discussed along with the statistical merit of various correlations.

II. MECHANICAL DAMAGING MECHANISMS IN CAVITATION AND LIQUID IMPINGEMENT.

A. Bubble Collapse Contours

As is well-known to cavitation researchers, it has been usually assumed from the time of Rayleigh's original bubble collapse analysis[1] until recent years that mechanical cavitation damage results from the imposition of essentially spherical shock waves promulgated through the liquid from the site of bubble collapse onto adjacent material surfaces. Theoretically, extremely high shock wave pressures are possible during collapse, and even more important, during subsequent rebound. This is true as recent numerical

studies have shown, even when the real fluid properties of compressibility and viscosity are considered[2, 3]. In addition, it is to be expected on theoretical grounds that the bubble centroid will move appreciably toward an adjacent surface during collapse[4, 5] so that the shock wave attenuation to be expected if the bubble center were stationary[2, 3] is reduced. However, the probable importance of this mode of collapse and damage in real flow situations is greatly reduced in the author's opinion by the fact that it requires a very large ratio, about 10^3 to 10^4 [3] between initial and final bubble radius to generate shock wave pressures of the magnitude necessary to explain observed pitting in strong materials. Recent experimental evidence, some of which is briefly reviewed below, indicates the improbability of such collapse radius ratios in real flow situations, as well as the likelihood of the production of damage in many situations by a liquid microjet which forms as a result of the asymmetric nature of bubble collapse in real situations. In those cases where cavitation damage is the result of microjet impingement it is clearly closely analogous to liquid drop or jet impact damage, except perhaps for the effect of scale, i.e., the drop or jet has a diameter which is probably many times greater than that of the microjet in cavitation. It is then probable that the microjet velocity must be greater than that in the impact experiments if damage to equally hard materials, as is observed, is to occur.

The collapse of a cavitation bubble through the radius ratio necessary to produce the observed pitting requires that a high degree of spherical symmetry exist. It has been shown theoretically[6] that a spherical collapse is unstable even if asymmetric influences are minimal. In an actual flow situation involving cavitation damage, very strong asymmetries are caused by the proximity of a wall (necessary if damage is to occur), pressure gradients, velocity gradients, influences of turbulence, etc. Thus a spherical collapse

through more than a small radius ratio is unlikely before a microjet develops. This has been shown experimentally to be the case by various previous investigators[7, 8, 9, 10, etc.]. Fig. 1 shows recent frames from a high-speed motion picture sequence obtained in our laboratory showing a spark-generated bubble in a water venturi collapsing adjacent to a knife-edge of aluminum, which is oriented parallel to the flow. It is clear that the effective radius decreases by a factor of about 10 before a microjet is formed. This then impacts the soft aluminum at about 100 m/s, which is sufficient to cause a crater. The bubble centroid moves appreciably toward the wall during this sequence. After the impact the bubble "rebounds" to an appreciable fraction of its initial size. It is possible to locate the single crater formed by such a single microjet impact. In this experiment, where the important parameters are under very close control, it is thus possible to produce a crater with a single bubble implosion. Actual flow experiments[11, e.g.] with random cavitation fields normally showing a ratio of 10^4 to 10^5 between bubbles observed to collapse adjacent to surface and individual craters actually formed. The fact that such a large ratio is found for a random cavitation field, but that for carefully controlled collapse a unity ratio can be obtained (Fig. 1) is indicative of a very great sensitivity of damaging potential to precise bubble collapse parameters. Such a high level of sensitivity seems much more likely if the bubble collapses in the microjet mode rather than with spherical symmetry, since bubble orientation then becomes a variable parameter, in addition to bubble size, position, and gas content.

B. Non-Photographic Experimental Evidence of Damaging Bubble Collapse Mode

As mentioned above, Fig. 1 shows a spark-generated bubble collapsing in a microjet mode with the production of a crater in the adjacent aluminum wall. However, a second crater is also

produced directly beneath the spark electrodes, presumably by the shock waves radiated from the growing bubble. Thus this experiment also shows that the shock wave mechanism, at least for a growing bubble, can produce damage, and in fact provides a method for studying either shock or jet produced damage. In flowing fields, however, it seems unlikely for the reasons already discussed that bubble collapse can proceed in such a manner that shock wave damage will be a predominant mechanism. There is at present no direct proof of this statement, but some experimental evidence in its support from our laboratory is shown in Figs. 2 and 3.

Fig. 2 shows craters produced by cavitating water on a cadmium-plated stainless steel cylinder placed across the diffuser of a cavitating venturi. The cadmium thickness is 0.6 microns (0.6×10^{-3} mm) and the full crater diameters are about 0.1 mm. The cadmium-plate is completely removed from the central region (about 1/2 the full diameter) so that the under-lying stainless steel is exposed. This region is surrounded by an annular area from which the cadmium is partly removed. This damage disposition suggests the impact of a microjet which accelerates radially after impact (a common observation for the impact of actual liquid jets[12]), and washes away the cadmium plate. However, we found in experiments where hard steel balls were shot at the surface (about 100 m/s) that a spherical shock front as thus provided would merely press the cadmium down into the surface rather than remove it.

Presumably the cavitation craters were produced by a microjet of diameter less than that of the central region. If the diameter of the jet were about 1/2 that of the central region, the jet diameter would be about 0.02 mm (20 microns). The diameter of the microjet shown in Fig. 1 is about 60 microns, but this spark-generated bubble is larger than typical cavitation bubbles. Previous comparisons we have made between actual jet and cavitation pit profiles in stainless steel indicated a probable microjet diameter of 1-25 microns.[11] These various

estimates probably cover the actual range of microjet diameters in typical flow cases.

Fig. 3 shows a cavitation crater produced in plexiglas in the cavitating water venturi. This crater has an overall diameter of about 12 microns, with a central impact region of about 4 micron diameter. Assuming that the jet which produced this crater had a diameter no more than that of the central region, the microjet diameter would be about 4 microns, i.e., of the same general order of magnitude obtained from the previously discussed estimates.

The plexiglas crater shown in Fig. 3 is very similar to damage observed in plexiglas from the impact of large-scale droplets or jets. Fig. 4 shows such a crater of about 0.8 mm diameter. As is typical for plexiglas, there is a central relatively undamaged area directly under the droplet impact and the droplet diameter is about that of this region. Since this material is stronger in compression than tension, failure does not occur in the region of impact where the stress is compressive, but in a region at a considerably larger diameter where tensile stresses predominate. The very strong similarity in form between the very small cavitation pit and the much larger droplet impact pit in the plexiglas is evident, thus indicating the strong likelihood that the cavitation pit was formed by microjet impingement rather than shock wave imposition. Since the impact region of the cavitation pit is indeed damaged, whereas it is not damaged in the case of the droplet impact (about 300 m/s), the cavitation microjet impact velocity must be somewhat greater than this value in this case.

Another segment of the experimental evidence from this laboratory favoring the theory of microjet rather than shock wave cavitation damage is the fact[11] that the craters from individual bubble collapse on steels in our venturi were observed to be "tipped", i.e., their axis was not perpendicular to the surface. Similar

non-symmetrical craters are observed in the plexiglas tests (Fig. 5). This type of crater could easily be formed with a non-perpendicular jet impact. In fact this has been observed with larger drop impacts on plexiglas [12]. However, it seems intuitively unlikely that such craters could be formed by the imposition of spherical shock waves, the local sound velocity being much greater than the flow velocities in the vicinity of the crater.

III. CORRELATION OF DAMAGE RATES WITH MECHANICAL MATERIAL PROPERTIES

A. General Considerations

Many papers have been published over the last 30 to 40 years on the relationship between cavitation or liquid impingement damage and material mechanical properties. However, no good correlation, valid over a broad range of materials or test parameters has emerged. This lack of a precise correlation with mechanical properties of materials is no doubt due to many factors among which can be included:

a) Corrosion effects are always present to some extent;

b) Most mechanical properties are measured under semi-static conditions, but failure under cavitation or liquid impingement occurs in a few microseconds;

c) Cavitation or impingement attack does not closely resemble any of the laboratory-induced failures used to measure various mechanical properties.

d) The modes of failure under cavitation or impingement differ drastically between even metallic materials, and even for the same material depending upon the intensity of attack.

Nevertheless, it is useful to attempt a simple correlation over as broad a range of material and test conditions as possible to

obtain an idea of the possible precision and generality of such fits. As explained in the following we have recently completed such an attempt.

B. Mechanical Property Correlations

Since it seems likely that the basic mechanical damaging processes in cavitation are very similar to those in droplet or jet impingement, we have used a data set which includes vibratory cavitation tests (with both vibrating specimen and stationary specimen) from our own laboratory, venturi cavitation tests[13] from the Indian Institute of Science, Bangalore, India, and rotating arm and disc impact tests from Dornier Systems[14] and Electricite de France[15] In all cases the material mechanical properties are well known, and in many cases identical materials were used which were cut from the same piece of stock. Common materials linking all data sets existed, and the volume loss rates per unit exposed area (MDPR) were normalized to those common materials. In all cases the maximum volume loss rates were used. The resulting 33 normalized MDPR values[16] and all pertinent mechanical properties are listed in Table 1. The last two items, Stellite 6-B and a tool steel, were not considered in the correlation since their properties differ very substantially from those of the other materials and therefore they appear to be special cases.

It is recognized that for any such data set it would be possible to generate a good correlating function in terms of any selected mechanical property or group of properties if sufficient degrees of freedom in the fitting function were used, i.e., a power series with a large number of terms might be used. However, since the physical model behind such a polynomial fit would be weak, it is not likely that the resulting correlation would fit new data points. For this reason, it was desired to use as rational and simple a model as possible. It was thus assumed that the maximum

volume loss rate would be inversely proportional to the energy required to remove a unit volume from the material. Thus it was desired to find the best material property which could be derived from the conventional mechanical properties and would have units of energy per unit volume. Our own past experience in this regard[17], as well as suggestions of other investigators,[18, 19] led us to assume that the mechanical energy property to be investigated would be a combination of ultimate resilience UR = (ultimate tensile strength)^2/2(elastic modulus), as suggested by Hobbs,[18] and strain energy to failure SE [19, etc.], which is the total area under conventional stress-strain curve. Ultimate resilience is the area under the stress-strain curve if failure were entirely elastic, i.e., if brittle failure occurred. Observation of damage surfaces leads to the conclusion that this may be the case. We thus attempted a least mean square regression analysis fit of the type

$$\frac{1}{\text{MDPR}} = C_o + C_1 \text{UR} + C_2 \text{SE} \qquad (1)$$

Eq. (1) was investigated by computer, with the following results:

a) The correlation coefficient with SE alone was very poor compared to that with UR.

b) The correlation coefficient with UR and SE together was only slightly better than that with UR alone. Since in addition SE is much more difficult to evaluate for many materials of interest than is UR, SE was henceforth dropped from the correlation.

c) The best fit value for C_o was close to zero, so that its inclusion improved the fit only slightly. Hence C_o also was dropped.

d) If UR is raised to an arbitrary exponent in the remaining relation, the best value for this exponent is very close to unity.

It thus appears that the physics of the model, which assumes a first power energy relation, is essentially correct. Results (a), (b), and (c) above were previously reported[16].

As a result of our own work above, we recommended the simple relation, eq. (2), that reciprocal maximum volume loss rate is proportional to ultimate resilience

$$\frac{1}{MDPR} = C \cdot UR \qquad (2)$$

However, the fit is by no means precise. The correlation coefficient obtained was 0.811 and the standard error of estimate, taken as a factor of the actual value, 2.52.

Other papers appearing at approximately the same time or subsequently have suggested that improved correlations can be obtained in terms of UR x (Brinell hardness)[13] or UR x (elastic modulus)^2 [20]. We have investigated these suggested correlations for our own data set, and the results are shown in Table 2. The correlation coefficients are of the same order of magnitude but appreciably less than those for the simple UR relation, eq. (2), and the standard error of estimate factors considerably greater.

Fig. 6, 7, and 8 show the actual data, standard deviation cone, and best fit line.

IV. CONCLUSIONS

From this investigation we conclude the following:

a) The mechanical component of cavitation damage in flowing systems is most probably predominantly the result of microjet impact generated by the asymmetric collapse of bubbles

close to solid objects. The asymmetries are the result of the proximity of the object to be damaged, pressure gradients, velocity gradients, etc. Thus cavitation damage and droplet or jet impingement damage is basically very similar.

b) A precise correlation between cavitation and impingement damage rates and conventional material mechanical properties which will have general applicability to a broad range of materials, even if only metallic materials are considered, is not possible, for a standard deviation less than a factor of about 2.52. Certainly, individual materials, such as Stellite 6-B can differ from the prediction by a much larger factor ($\sim$10 for Stellite).

c) The best such correlation is in terms of the first power of ultimate resilience. Slight improvements may be possible in terms of more complex functions, but the improvement is not great.

V. BIBLIOGRAPHY

1. Lord Rayleigh, "On the Pressure Developed in a Liquid During the Collapse of a Spherical Cavity", Phil. Mag., 34, 94-98, 1917.

2. R. Hickling and M. S. Plesset, "Collapse and Rebound of a Spherical Cavity in Water", The Physics of Fluids, 7, 1, 6-19, 1964.

3. R. D. Ivany and F. G. Hammitt, "Cavitation Bubble Collapse in Viscous, Compressible Liquids -- Numerical Analysis", Trans. ASME, J. of Basic Engr., D, 87, 4, 977-985, 1965.

4. A. Shima, "The Behavior of a Spherical Bubble in the Vicinity of a Solid Wall", Trans. ASME, D, 90, 1, 75-89, 1968.

5. G. A. Khoroshev, "Influence of a Wall on the Collapse of Cavitation Bubbles", Inzhenero-fizicheskiy Zhurnal, 6, 1, 59-65, 1963.

6. M. S. Plesset and T. P. Mitchell, "On the Stability of the Spherical Shape of a Vapor Cavity in a Liquid", Quarterly Appl. Math., 13, 419-430, 1956.

7. T. B. Benjamin and A. T. Ellis, "The Collapse of Cavitation Bubbles and the Pressures Thereby Produced Against Solid Boundaries", Phil. Trans. Roy. Soc., A, 260, 1110, 221-240, 1966.

8. S. P. Kozirev, "On Cumulative Collapse of Cavitation Cavities", Trans. ASME, J. Basic Engr., D, 90, 1, 116-124, 1968.

9. S. P. Kozirev, "Collapse of Cavities Formed by Electrical Discharge in Liquid", Sov. Phys.-Doklady, 13, 11, 1168-1170, May 1969, (English trans.).

10. R. D. Ivany, F. G. Hammitt, and T. M. Mitchell, "Cavitation Bubble Collapse Observations in a Venturi", Trans. ASME, J. Basic Engr., D, 88, 3, 649-657, 1966.

11. M. J. Robinson, F. G. Hammitt, "Detailed Damage Characteristics in a Cavitating Venturi", Trans. ASME, J. Basic Engr., D, 89, 161-173, 1967.

12. A. A. Fyall, "Single Impact Studies with Liquids and Solids", Proc. 2nd Meersburg Conf. on Rain Erosion and Allied Phenomena, August,1967, edited A. A. Fyall and R. B. King, RAE, Farnborough, England.

13. R. C. Syamala Rao, N. S. Lakshmana Rao, K. Seetharamiah, "Cavitation Erosion Studies with Venturi and Rotating Disc in Water", ASME Paper 69-WA/FE-3, to be published Trans. ASME, J. Basic Engr.

14. G. Hoff, G. Langbein, H. Rieger, "Investigation of the Angle-Time Dependence of Rain Erosion", Prog. Report No. 62269-7-002050, Dornier Systems GmbH, March, 1968.

15. R. Canavelis, "Comparison of the Resistance of Different Materials with a Jet Impact Test Rig", HC/061-230-9, Electricite de France, Chatou, France, November,1967.

16. F. G. Hammitt, Y. C. Huang, C. L. Kling, T. M. Mitchell, L. P. Solomon, "A Statistically Verified Model for Correlating Volume Loss Due to Cavitation or Liquid Impingement", ASTM Symposium on Characterization and Determination of Erosion Resistance, June, 1969, to be published ASTM STP.

17. R. Garcia, F. G. Hammitt, "Cavitation Damage and Correlations with Materials and Fluid Properties", Trans. ASME, J. Basic Engr., D, 89, 4, 753-763, 1967.

18. J. M. Hobbs, "Experience with a 20-kc Cavitation Erosion Test", ASTM STP No. 408, 159-179, 1967.

19. A. Thiruvengadam, "A Unified Theory of Cavitation Damage", Trans. ASME, J. Basic Engr., D, 85, 3, 365-376, 1963.

20. F. J. Heymann, "Erosion by Cavitation, Liquid Impingement, and Solid Impingement", Engr. Report E-1460, Westinghouse Elec. Corporation, Dev. Engr. Dept., Lester, Pa., March 1968.

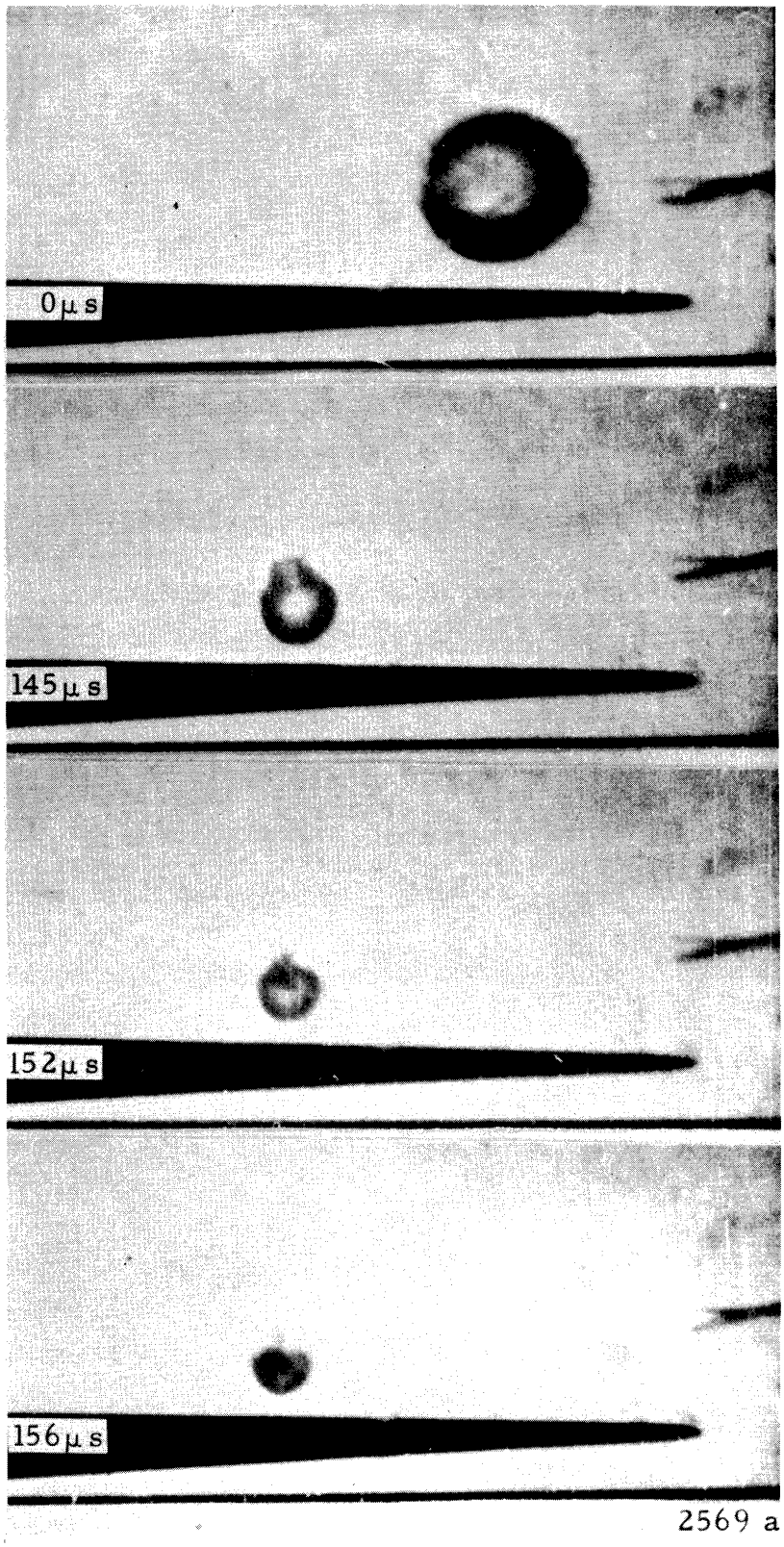

Figure 1. Selected Frames from a Sequence Taken at 550,000 Frames/Second of a Spark Generated Cavitation Bubble Near a Splitter in a Venturi, Exposure 1.8 μs/Frame, Flow Right to Left, Magnification 5 x.

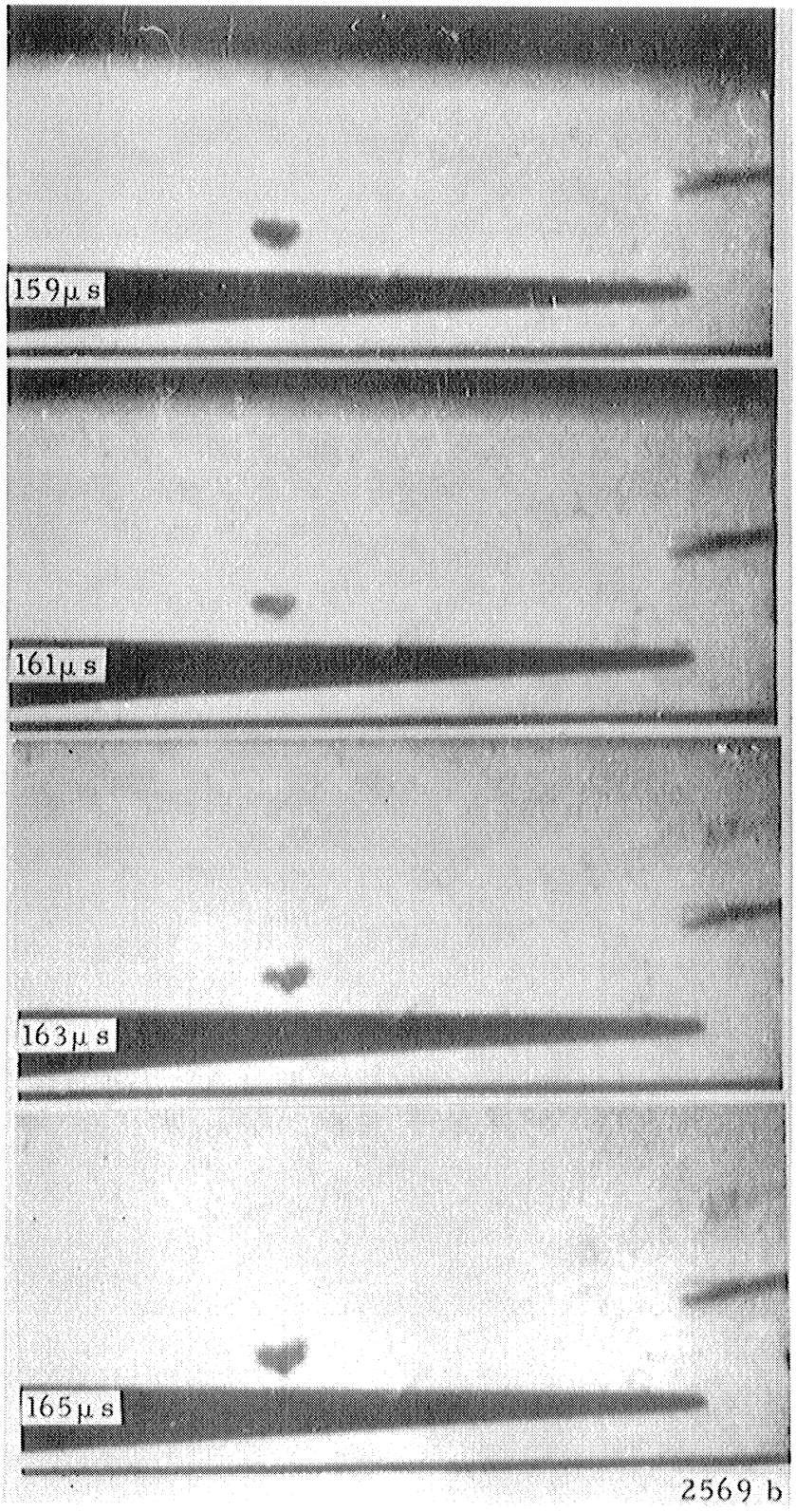
159μs
161μs
163μs
165μs
2569 b

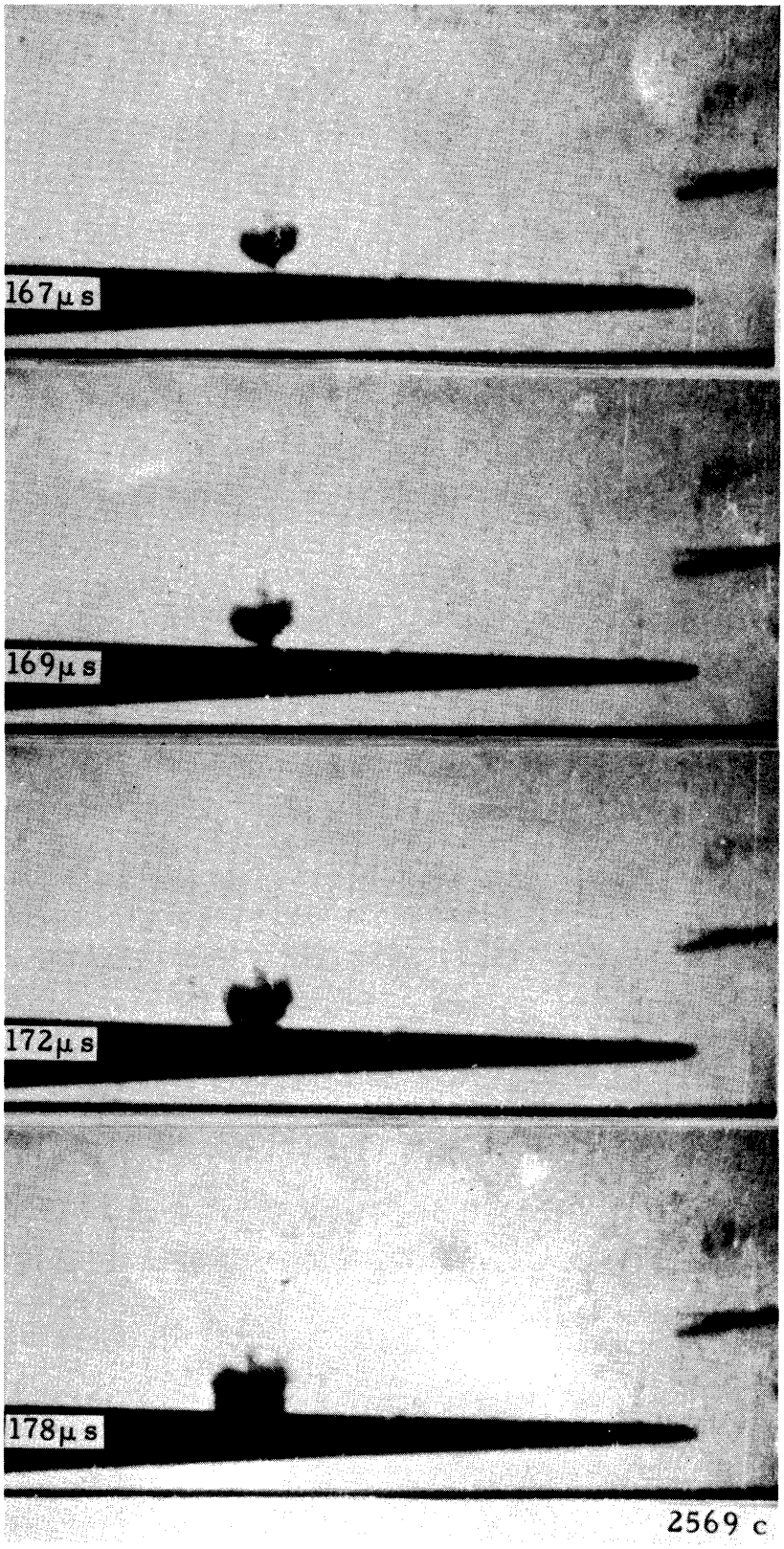
167μs
169μs
172μs
178μs
2569 c

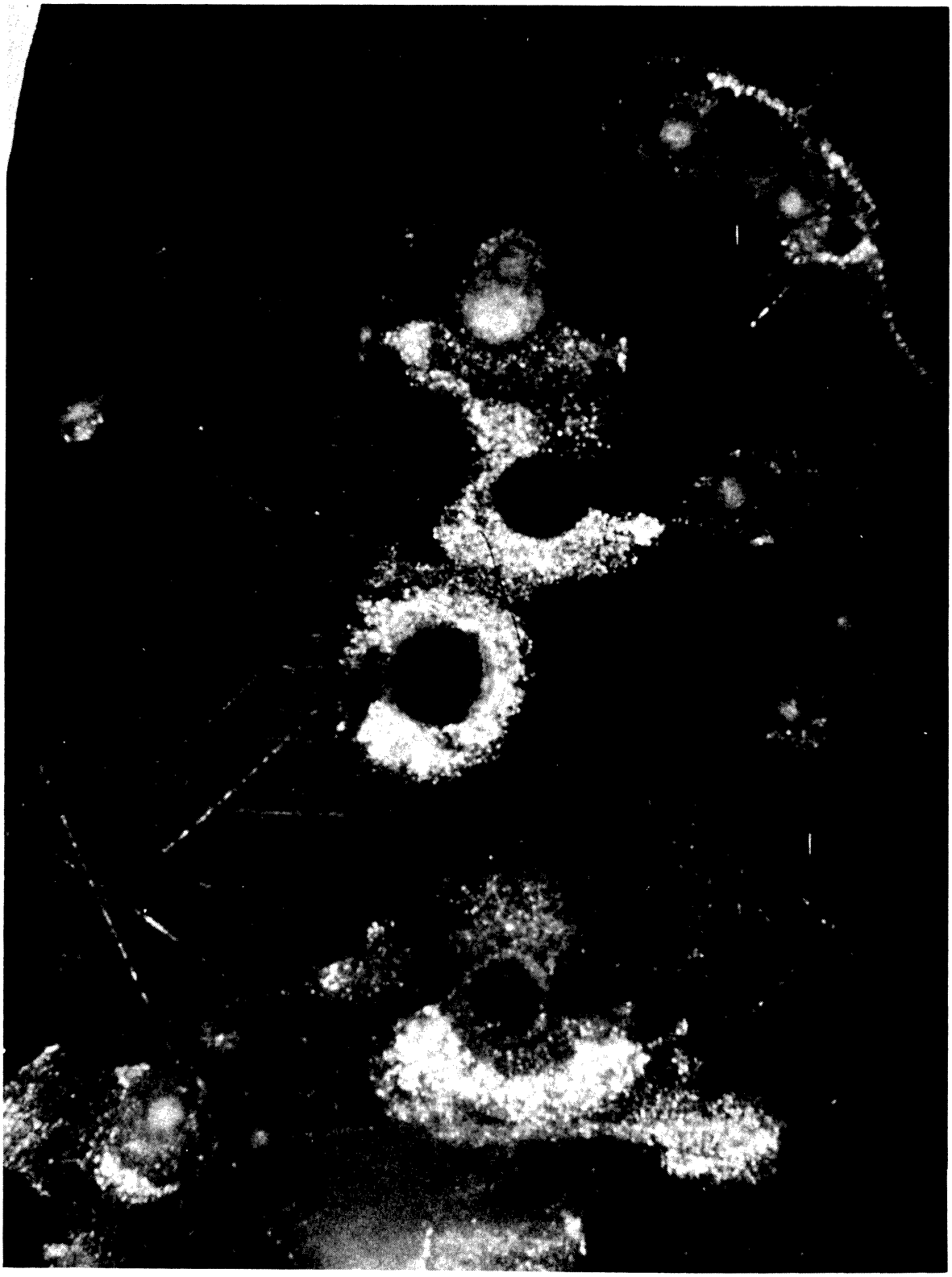

2443

Figure 2. Craters Produced by Cavitating Water on 0.6 μm Cadmium-Plated Stainless Steel, Magnification 180 x.

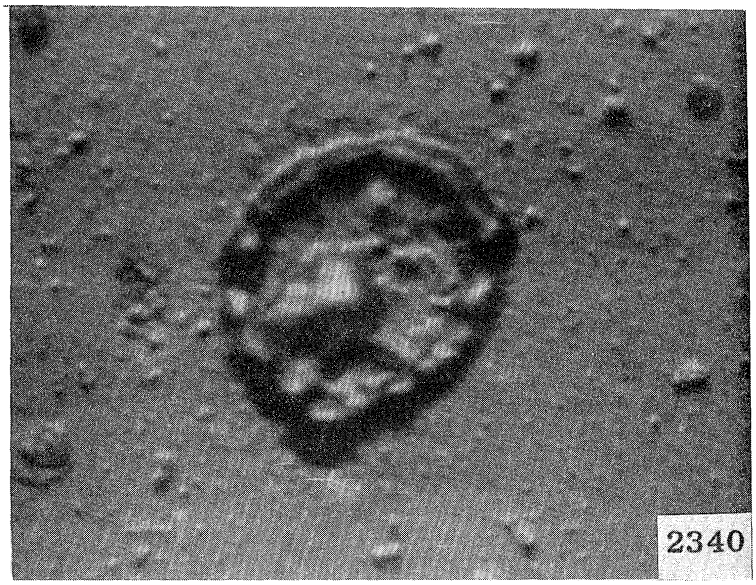

Figure 3. Crater Produced by Cavitating Water in a Venturi on Plexiglas, Magnification 4,000 x.

Figure 4. Water Droplet Impact Crater on Plexiglas, Magnification 100 x. (After A. Fyall, RAE, Farnborough, England).

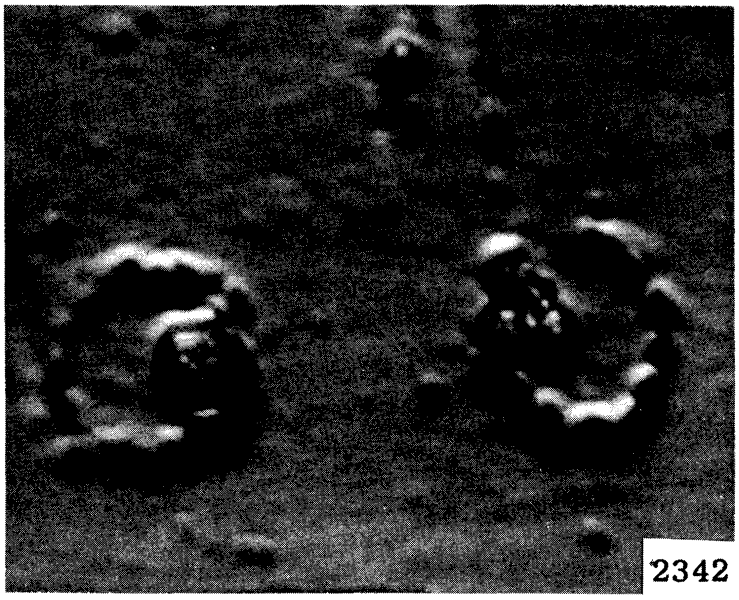

Figure 5. Non-Symmetric Craters Produced by Cavitating Water in a Venturi on Plexiglas, Magnification 4,000 x.

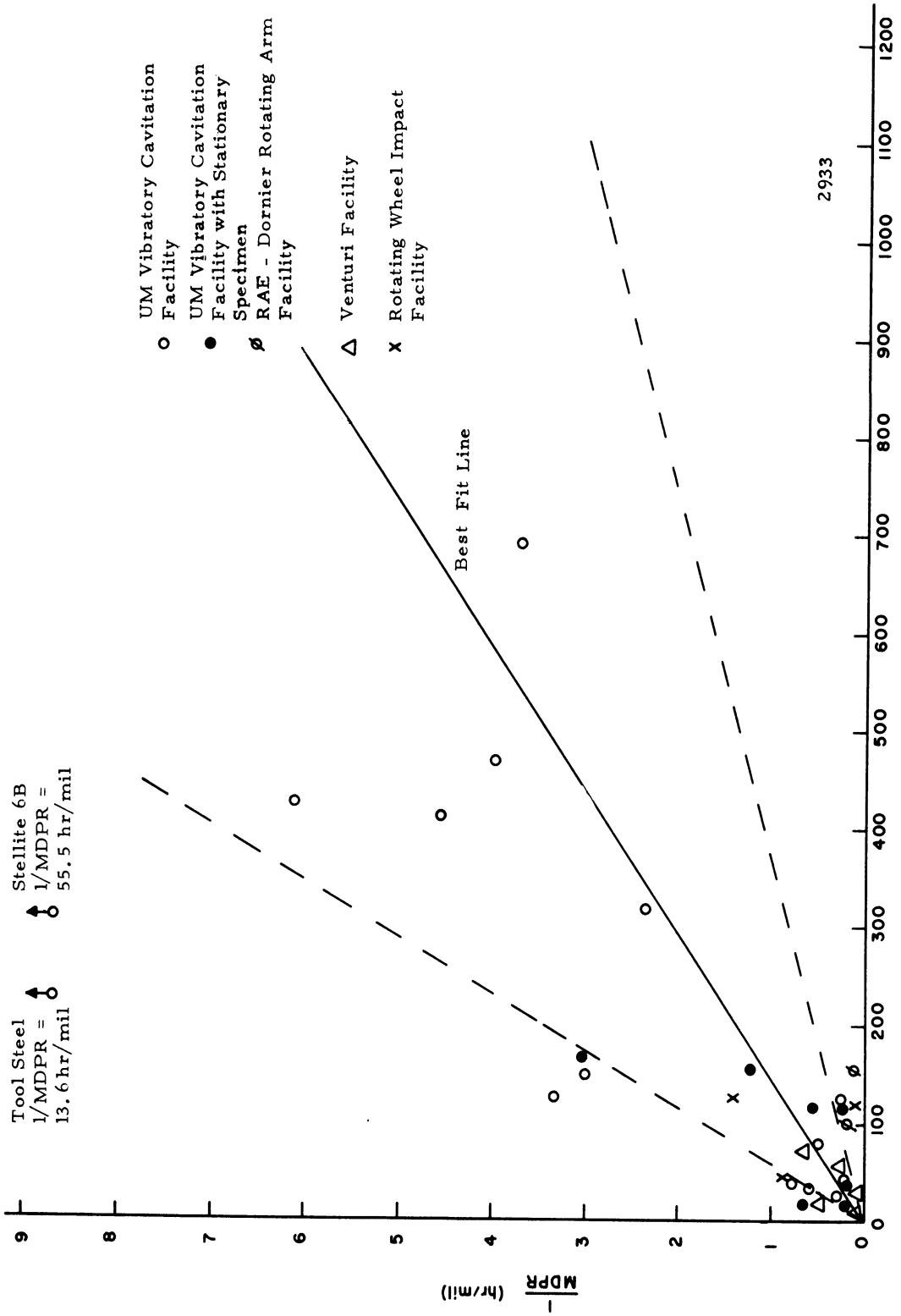

Figure 6. Best Fit Correlation and Standard Deviation Cone for 1/MDPR vs. Ultimate Resilience for 33 Materials.

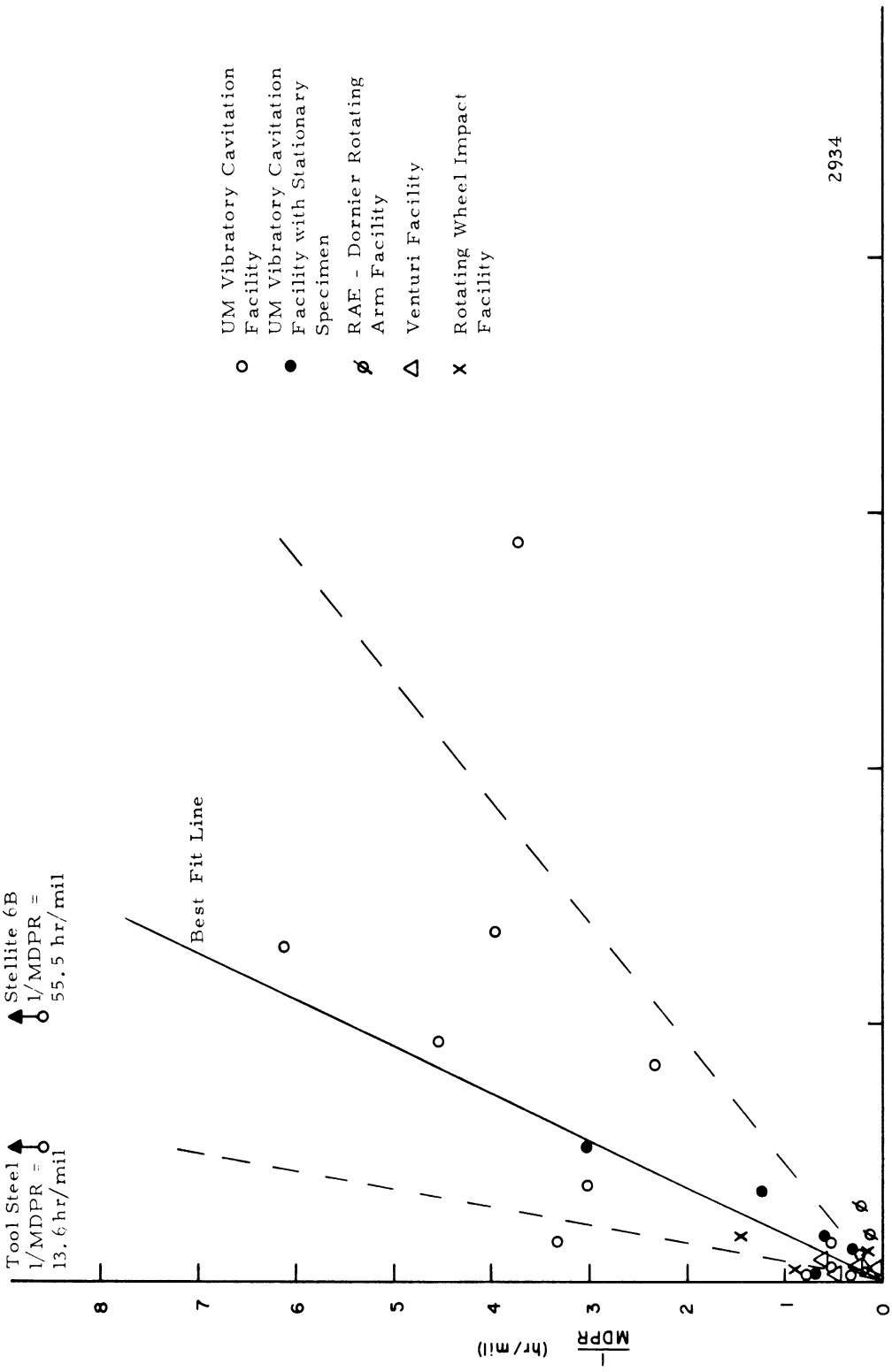

Figure 7. Best Fit Correlation and Standard Deviation Cone for 1/MDPR vs. UR x BHN for 33 Materials.

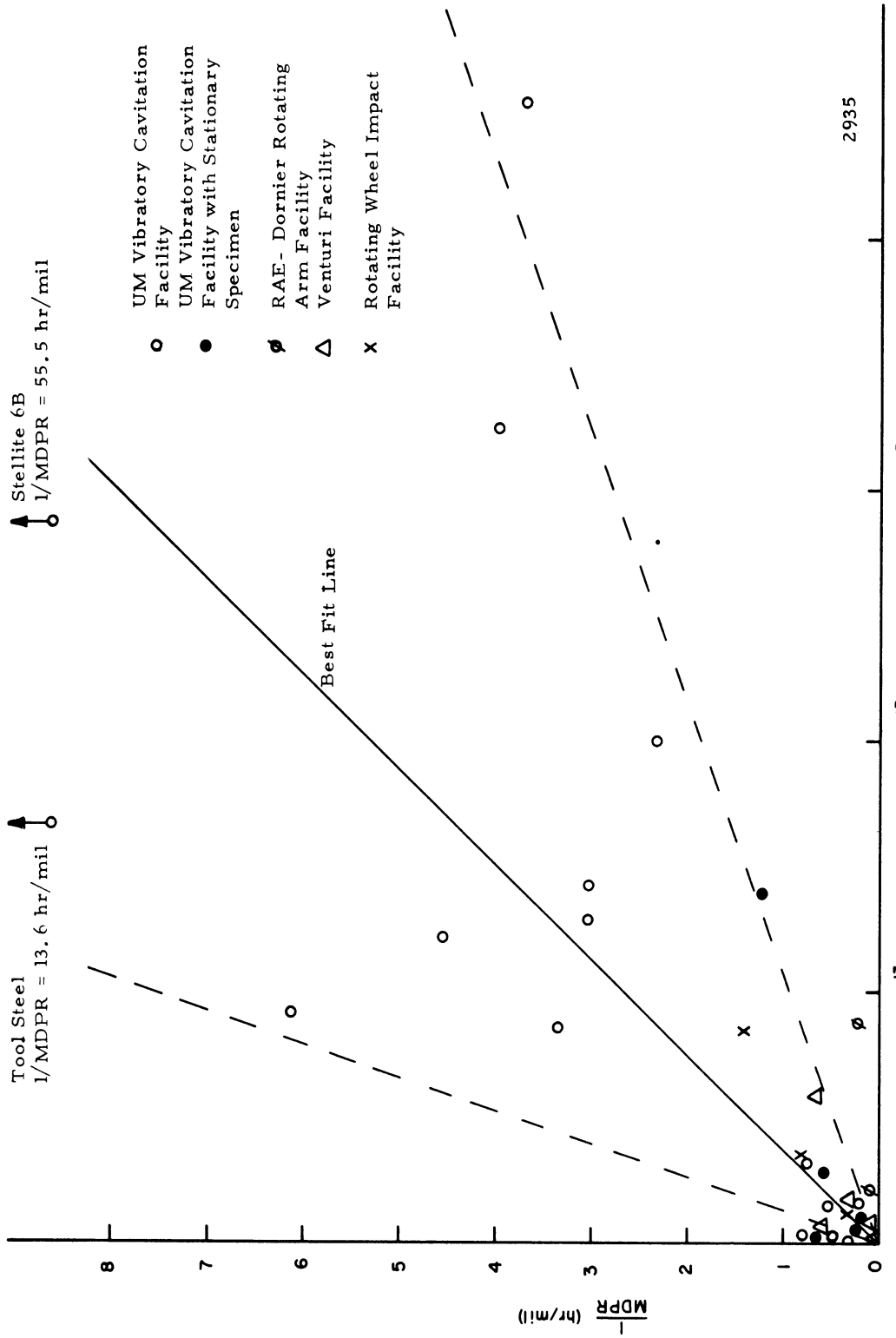

Figure 8. Best Fit Correlation and Standard Deviation Cone for $1/MDPR$ vs. $UR \times E^2$ for 33 Materials.

TABLE 1 Mechanical Properties of Materials in Data Set

	YS	TS	Y	EL	HARD	MDPR	UR	SE	NUR	NSE
BS1433 COPPER	0.300E 05	0.360E 05	0.180E 08	0.180E 00	0.900E 02	0.647E 01	0.360E 02	0.648E 04	1.000	1.000
STAINLESS STEEL 316	0.310E 05	0.813E 05	0.260E 08	0.690E 00	0.748E 02	0.301E 00	0.127E 03	0.561E 05	3.531	8.657
NICKLE 270	0.800E 04	0.488E 05	0.277E 08	0.610E 00	0.249E 02	0.128E 01	0.430E 02	0.298E 05	1.194	4.594
AL 6061	0.407E 05	0.475E 05	0.910E 07	0.220E 00	0.600E 02	0.436E 01	0.124E 03	0.104E 05	3.444	1.613
STAINLESS STEEL 304	0.647E 05	0.945E 05	0.290E 08	0.638E 00	0.237E 03	0.330E 00	0.154E 03	0.603E 05	4.277	9.304
BRONZE #1	0.243E 05	0.452E 05	0.128E 08	0.230E 00	0.189E 03	0.189E 01	0.798E 02	0.104E 05	2.217	1.604
BRONZE #2	0.790E 05	0.112E 06	0.147E 08	0.205E 00	0.304E 03	0.163E 00	0.426E 03	0.229E 05	11.834	3.537
BRONZE #3	0.880E 05	0.119E 06	0.172E 08	0.150E 00	0.225E 03	0.220E 00	0.411E 03	0.178E 05	11.410	2.752
BRONZE #4	0.190E 05	0.282E 05	0.121E 08	0.600E-01	0.152E 03	0.176E 01	0.329E 02	0.169E 04	0.913	0.261
BRONZE #5	0.105E 05	0.189E 05	0.558E 07	0.130E 00	0.974E 02	0.330E 01	0.320E 02	0.246E 04	0.889	0.379
BRONZE #6	0.162E 05	0.193E 05	0.711E 07	0.300E-01	0.152E 03	0.257E 01	0.262E 02	0.579E 03	0.728	0.089
STAINLESS STEEL #1	0.115E 06	0.157E 06	0.263E 08	0.220E 00	0.290E 03	0.252E 00	0.470E 03	0.346E 05	13.050	5.337
STAINLESS STEEL #2	0.186E 06	0.188E 06	0.257E 08	0.750E-01	0.418E 03	0.270E 00	0.691E 03	0.141E 05	19.189	2.179
STAINLESS STEEL #3	0.104E 06	0.126E 06	0.251E 08	0.195E 00	0.264E 03	0.430E 00	0.319E 03	0.247E 05	8.865	3.807
COPPER	0.282E 05	0.333E 05	0.160E 08	0.543E 00	0.968E 02	0.671E 01	0.347E 02	0.181E 05	0.963	2.790
BRASS(65-35)	0.489E 05	0.605E 05	0.157E 08	0.393E 00	0.146E 03	0.170E 01	0.117E 03	0.238E 05	3.238	3.669
MILD STEEL 1020	0.897E 05	0.965E 05	0.300E 08	0.259E 00	0.227E 03	0.808E 00	0.155E 03	0.250E 05	4.311	3.857
STAINLESS STEEL 304	0.410E 05	0.994E 05	0.290E 08	0.168E 00	0.315E 03	0.332E 00	0.170E 03	0.167E 05	4.732	2.577
ASTM B144(SAE660)	0.175E 05	0.225E 05	0.140E 08	0.173E 00	0.174E 03	0.147E 01	0.181E 02	0.389E 04	0.502	0.601
MAGNESIUM	0.241E 05	0.392E 05	0.650E 07	0.255E 00	0.885E 02	0.434E 01	0.118E 03	0.100E 05	3.283	1.543
ALUMINUM 3003-O	0.680E 04	0.159E 05	0.900E 07	0.541E 00	0.512E 02	0.304E 02	0.140E 02	0.860E 04	0.390	1.327
COPPER	0.300E 05	0.360E 05	0.180E 08	0.180E 00	0.900E 02	0.647E 01	0.360E 02	0.648E 04	1.000	1.000
CR-130 STEEL	0.290E 05	0.780E 05	0.290E 08	0.280E 00	0.255E 03	0.465E 01	0.105E 03	0.218E 05	2.914	3.370
AL ALLOY	0.450E 05	0.560E 05	0.100E 08	0.100E 00	0.114E 03	0.802E 01	0.157E 03	0.560E 04	4.356	0.864
ALUMINUM	0.150E 05	0.160E 05	0.900E 07	0.500E-01	0.270E 02	0.255E 02	0.142E 02	0.800E 03	0.395	0.123
COPPER	0.142E 05	0.310E 05	0.170E 08	0.500E 00	0.600E 02	0.824E 01	0.283E 02	0.155E 05	0.785	2.392
PHOSPHOR BRONZE	0.394E 05	0.416E 05	0.150E 08	0.110E 00	0.950E 02	0.440E 01	0.577E 02	0.458E 04	1.602	0.706
BRASS	0.157E 05	0.260E 05	0.160E 08	0.530E 00	0.150E 03	0.200E 01	0.211E 02	0.138E 05	0.587	2.127
MILD STEEL	0.484E 05	0.650E 05	0.280E 08	0.600E-01	0.950E 02	0.236E 01	0.754E 02	0.390E 04	2.096	0.602
STAINLESS STEEL	0.354E 05	0.930E 05	0.280E 08	0.570E 00	0.170E 03	0.653E 00	0.154E 03	0.530E 05	4.290	8.181
STAINLESS STEEL 316	0.310E 05	0.813E 05	0.260E 08	0.690E 00	0.748E 02	0.713E 00	0.127E 03	0.561E 05	3.531	8.657
NICKLE 270	0.800E 04	0.488E 05	0.277E 08	0.610E 00	0.249E 02	0.126E 01	0.430E 02	0.298E 05	1.194	4.594
AL 6061	0.407E 05	0.475E 05	0.910E 07	0.220E 00	0.600E 02	0.436E 01	0.124E 03	0.104E 05	3.444	1.613
STELLITE 6-B	0.710E 05	0.138E 06	0.304E 08	0.210E 00	0.322E 03	0.180E-01	0.313E 03	0.290E 05	8.728	4.475
TOOL STEEL #1	0.540E 05	0.110E 06	0.275E 08	0.175E-01	0.235E 03	0.730E-01	0.220E 03	0.193E 04	6.111	0.298

YS = Yield Strength (psi)

TS = Tensile Strength (psi)

Y = Elastic Modulus (psi)

EL = Elongation (%)

HARD = Brinell Hardness

MDPR = Maximum Mean Depth of Penetration Rate (mils/hr) (All values are corrected to U. M. vibratory facility)

UR = Ultimate Resilience = $TS^2/2E$ (psi)

SE = Strain Energy to Failure = TS x E (psi)

NUR = Ultimate Resilience normalized to BS 1433 Copper

NSE = Strain Energy normalized to BS 1433 Copper

TABLE 2

Correlating Relation	Correlation Coefficient	Standard Error of Estimate Factor
$\frac{1}{MDPR} = C\,(UR)$	0.811	2.52
" $= C\,(URxBHN)$	0.716	2.57
" $= C\,(URxE^2)$	0.684	2.86
" $= C\,UR^b$ $(b = 0.9985)$	0.811	2.57
" $= C\,(SE)$	0.498	3.30
" $= C\,(Hardness)$	0.742	2.75